Supplementary information: charge density waves in cuprate superconductors beyond the critical doping

(Dated: February 22, 2021)

SUPPLEMENTARY NOTE 1: TIGHT BINDING MODEL

The band-dispersion shown in the main text has the form [1, 2]

$$\begin{aligned}\epsilon_k =& \mu - 2t[\cos(k_x a) + \cos(k_y a)] - 4t_1 \cos(k_x a)\cos(k_y a) \\ & - 2t_2[\cos(2k_x a) + \cos(2k_y a)] - 4t_3[\cos(2k_x a)\cos(k_y a) \\ & + \cos(k_x a)\cos(2k_y a)] - 4t_4 \cos(2k_x a)\cos(2k_y a)\end{aligned} \tag{1}$$

where t and t_i ($i = 1, 2, 3, 4$) are hopping parameters. Their relative ratios are $t_1/t = -0.136$, $t_2/t = 0.068$, $t_3/t = 0$, $t_4/t = -0.02$, and $t = 1720$ meV. Fermi-surface changes with doping are achieved by tuning the chemical potential, μ, while keeping the hopping parameters unchanged.

SUPPLEMENTARY NOTE 2: FITTING OF THE CDW PEAK

Following previous studies [3, 5–7], the CDW peaks were fitted by a Lorentzian-squared function

$$I_{\mathrm{CDW}}(T) = I_{\mathrm{BG}}(T) + \frac{I_0(T)}{\left(1 + \left[\frac{Q - Q_0(T)}{\Gamma}\right]^2\right)^2} \tag{2}$$

where $I_{\mathrm{BG}}(T)$ is a polynomial background, which we found to be of third order in the present dataset. The relation between Γ, (HWHM), and in-plane correlation length, $\xi_{\parallel}$, is given by $\mathrm{HWHM} = \Gamma\sqrt{(\sqrt{2}-1)}$ where $\Gamma = 1/\xi_{\parallel}$. In Fig. 2 of the main text, we show representative fittings for scans along $\boldsymbol{Q}_{\mathrm{CDW}}$ (longitudinal scans). Representative fittings for scan perpendicular to $\boldsymbol{Q}_{\mathrm{CDW}}$ (transverse scan) are shown in Supplementary figure 2. We used two Lorentzian-squared peaks to fit transverse scans in LSCO12 due to the known splitting of CDW peaks are known to split at this concentration [3, 4]. The HWHMs that are extracted from different transverse and longitudinal scans agree within 5% with respect to averaged value.

SUPPLEMENTARY NOTE 3: ABSENCE OF CDW SIGNAL IN LSCO25

Supplementary figure 1 shows K and H of LSCO25 scans near possible CDW wavevectors. Within our experimental uncertainty, we do not observe any CDW superlattice peaks at $T = 15$ K $\approx T_{\mathrm{SC}}$. This was observed consistently

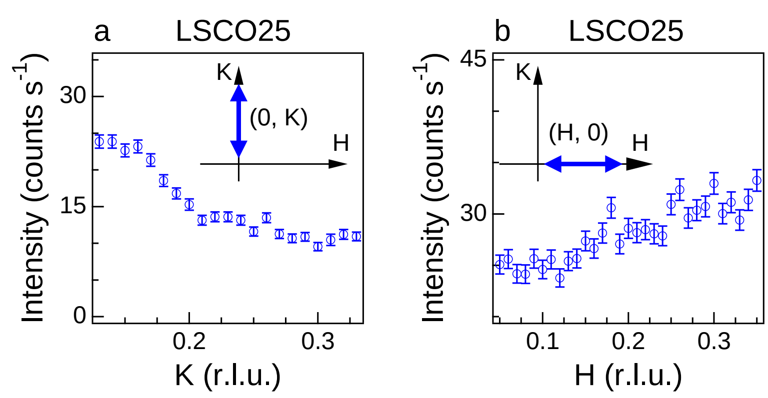

Supplementary figure 1. **Absence of a CDW peak in LSCO25.** (a) and (b) shows scans along the K and H directions, respectively. The scans are taken at $L = 12.5$. The in-plane scan trajectories are shown as insets to each panel. The data were taken at 15 K, just above T_{SC}. Errorbars are one standard deviation based on Poissonian statistics.

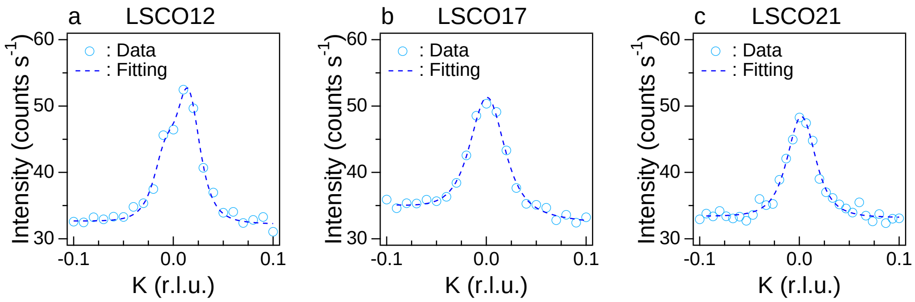

Supplementary figure 2. **Fitting of the CDW peak.** Representative Lorentzian-squared fits (Eq. 2 of the CDW peak perpendicular to $\boldsymbol{Q}_{\mathrm{CDW}}$ near T_{SC} are shown in (a)-(c). Note that the data for LSCO12 is composed of two peaks, as previously demonstrated [3, 4]. Errorbars are one standard deviation based on Poissonian statistics.

with different samples and different beamlines. The absence of a CDW points towards a possible connection between CDW correlations and non-Fermi-liquid transport as both seem to disappear concurrently (see also Appendix V) .

SUPPLEMENTARY NOTE 4: CDW INTENSITY

Assuming a weak interplanar CDW correlation, the integrated x-ray scattering intensity, $I^{\mathrm{int}} = I_0$ HWHM^2 $= I^{\mathrm{peak}}(\sqrt{2}-1)\Gamma^2$, is used to estimate the magnitude of the CDW order parameter [8]. Former x-ray studies found that the CDW magnitude in LSCO12 is about four times smaller than in $La_{1.875}Ba_{0.125}CuO_4$ and $YBa_2Cu_3O_{6.612}$ (YBCO) [8]. This is based on a direct comparison of scattering intensity in reflection using 9 keV x-rays. We note that LSCO has a shorter x-ray penetration depth of between 6.70-6.9 μm (dependent on doping) compared to 8.2 μm in YBCO. We remind the reader that LSCO also has fewer CuO_2 planes per unit volume compared to YBCO, such that approximately three times fewer CuO_2 planes are illumined in LSCO compared to YBCO. In this study, we use the same LSCO12 sample as previously [3]. The comparable CDW peak intensity and correlation length confirms that the CDW order parameter is of substantial size throughout the phase diagram (see Fig. 4 of the main text) and is expected to have an appreciable effect on the transport properties.

As we discussed in the main text, I^{int} also varies with doping. Based on the fits shown in Supplementary figure 3 of the main text, we find intensity ratios of 8:7:1 at T_{SC} for $x = 0.12$, 0.17, and 0.21. The magnitudes of the CDW order parameter are estimated based on data at $T = T_{\mathrm{SC}}$. The appreciable reduction of I^{int} in LSCO21 occurs close to the crossover from strange metal to Fermi liquid phase at low temperature.

SUPPLEMENTARY NOTE 5: RECOVERY OF QUASI-PARTICLE COHERENCE IN LSCO25

The ARPES intensity map of LSCO25 at E_F is shown in Supplementary figure 3(a). In agreement with previous studies [2, 9], well-defined quasiparticles are recovered in this heavily overdoped sample as shown in Supplementary figure 3(b)&(c). Near E_F, the quasiparticle scattering rate is given by $\mathrm{Im}\Sigma(k,\omega) = \frac{1}{2}\hbar v_F \Delta k(\omega)$, where $\mathrm{Im}\Sigma(k,\omega)$ is the imaginary part of the self-energy, v_F and ω are the Fermi velocity and the binding energy, respectively [10]. $\Delta k(\omega)$ can be extracted by fitting the momentum distribution curve (MDC) with a Lorentzian function

$$\Gamma^{\mathrm{MDC}}(k,\omega) = I_{\mathrm{BG}} + \frac{I_0(\omega)}{(k-k_0)^2 + (\Delta k)^2}, \tag{3}$$

where $I_{\mathrm{BG}}(\omega)$ and $I_0(\omega)$ are constants at fixed ω. Supplementary figure 3(c) shows the extracted $\Delta k(\omega)$, which can be further fitted with $a + b\omega^2$, as expected for a Fermi-liquid. One can also directly observe the emergence of a coherent quasiparticle peak the LSCO25 energy distribution curve (EDC) that was not present when compared to an LSCO12 EDC at a nearby E_F.

[1] Horio, M. *et al.* Three-dimensional Fermi surface of overdoped La-based cuprates. *Phys. Rev. Lett.* **121**, 077004 (2018).

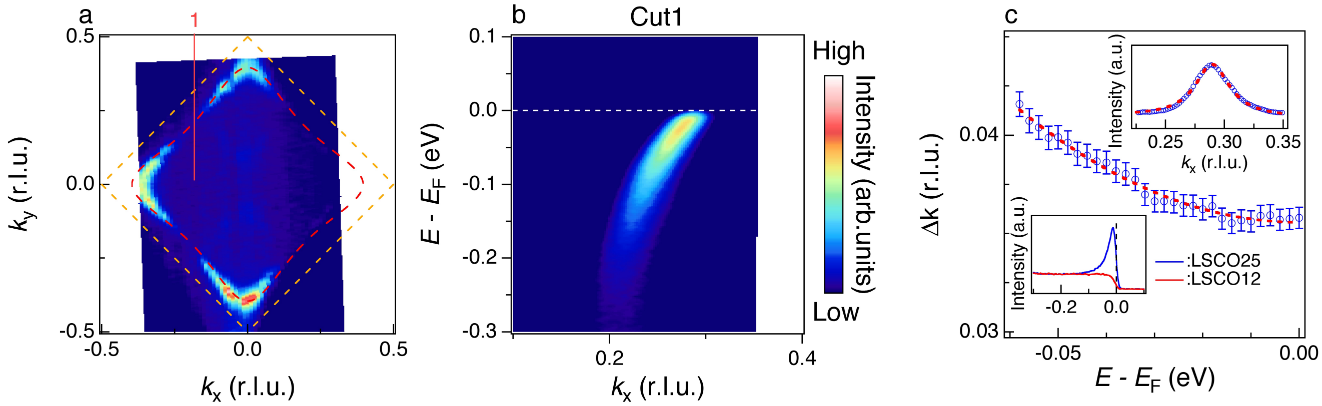

Supplementary figure 3. **The electronic structure of LSCO25.** (a) ARPES intensity map at E_F obtained by integrating the spectra in a ±10 meV energy window with respect to E_F. (b) Band dispersion along the red line shown in (a). (c) Display fits to the energy and momentum distribution curves (MDCs/EDCs). The upper panel shows the MDC (blue points) and a fit to a Lorentzian-function (Eq. 3) (red dashed curve) at E_F. The extracted MDC-width, Δk, is plotted as function of energy in the main panel of (c), which shows a ω^2-dependence, which is consistent with Fermi liquid behavior. The red-dashed curve shown in the main panel of (c) is a fit of the extracted Δk using a quadratic function, $a + b^2$. The bottom-left panel compares EDCs of LSCO12 (red) and LSCO25 (blue) at representative k_F, which are close in momentum space. Errorbars are one standard deviation derived from least-squares fitting.

[2] Chang, J. *et al.* Anisotropic breakdown of fermi liquid quasiparticle excitations in overdoped $La_{2-x}Sr_xCuO_4$. *Nat. Commun.* **4**, 1–5 (2013).

[3] Thampy, V. *et al.* Rotated stripe order and its competition with superconductivity in $La_{1.88}Sr_{0.12}CuO_4$. *Phys. Rev. B* **90**, 100510 (2014).

[4] Wen, J.-J. *et al.* Observation of two types of charge-density-wave orders in superconducting $La_{2-x}Sr_xCuO_4$. *Nat. Commun.* **10**, 3269 (2019).

[5] Wilkins, S. B. *et al.* Comparison of stripe modulations in $La_{1.875}Ba_{0.125}CuO_4$ and $La_{1.48}Nd_{0.4}Sr_{0.12}CuO_4$. *Phys. Rev. B* **84**, 195101 (2011).

[6] Chen, X. M. *et al.* Remarkable stability of charge density wave order in $La_{1.875}Ba_{0.125}CuO_4$. *Phys. Rev. Lett.* **117**, 167001 (2016).

[7] Miao, H. *et al.* High-temperature charge density wave correlations in $La_{1.875}Ba_{0.125}CuO_4$ without spin–charge locking. *Proc. Natl. Acad. Sci. U.S.A.* **114**, 12430–12435 (2017).

[8] Thampy, V. *et al.* Comparison of charge modulations in $La_{1.875}Ba_{0.125}CuO_4$ and $YBa_2Cu_3O_{6.6}$. *Phys. Rev. B* **88**, 024505 (2013).

[9] Yoshida, T. *et al.* Electronlike fermi surface and remnant $(\pi, 0)$ feature in overdoped $La_{1.78}Sr_{0.22}CuO_4$. *Phys. Rev. B* **63**, 220501 (2001).

[10] Valla, T. *et al.* Evidence for quantum critical behavior in the optimally doped cuprate $Bi_2Sr_2CaCu_2O_{8+\delta}$. *Science* **285**, 2110–2113 (1999).